https://doi.org/10.5194/egusphere-2026-3777
Preprint. Discussion started: 11 August 2026

An analytical formulation of optical inversion modeling of aerosol mixing state using AeroMix v1.0.1

Sam P. Raj[1] and Puna Ram Sinha[1]

[1]Department of Earth and Space Sciences, Indian Institute of Space Science and Technology Thiruvananthapuram, 695547, India

Correspondence: Puna Ram Sinha (prs@iist.ac.in)

Abstract. Accurate determination of the aerosol mixing state is indispensable in reducing uncertainties in the assessment of aerosol direct and indirect effects. However, the characterization of mixing state is often limited by the scarcity of direct measurements of aerosol chemical composition and their morphology. Thus, previous studies have largely relied on heuristic approaches to infer mixing states from optical measurements, which are generally deemed only as probable mixing states due to a lack of uncertainty quantification. To address this gap, this study formulates an optical inversion framework to infer aerosol mixing states and composition, explicitly characterizing the inherently ill-posed and ill-conditioned nature of the inversion problem. This formulation leverages the scalability of the AeroMix model in simulating optical properties of complex aerosol mixtures constituted by an arbitrary number of externally mixed and core-shell mixed aerosol components. Recognizing that standard optimization techniques cannot resolve this ill-posed system deterministically, the inversion framework is reframed as a system of linear inequalities. This approach geometrically bounds the feasible solution space as the boundary of a convex polytope. This theoretical confinement is further evaluated and empirically illustrated using simulated aerosol mixtures, confirming that all physically valid solutions strictly reside on the boundary facets of the formulated convex polytope. By transitioning from heuristic methods to an analytical geometry framework using AeroMix, this study establishes a rigorous foundation for the probabilistic determination of aerosol mixing states from widely available optical measurements.

1 Introduction

The accurate determination of aerosol mixing state is critical for reducing uncertainties in radiative forcing and cloud-condensation nuclei concentration estimates (Lesins et al., 2002; McFiggans et al., 2006). However, this remains a challenge due to the impracticality of obtaining direct, single-particle measurements at high spatiotemporal resolutions. Consequently, equivalent aerosol mixing states and chemical compositions are largely inferred from widely available, standardized optical measurements using optical inversion modeling techniques. This methodology is fundamentally a closure study utilizing a forward Mie model, where the objective is to achieve closure between modeled and measured optical properties by identifying a physically realistic aerosol mixture that best matches the measurements at a given location (Raj et al., 2024).

Earlier optical closure studies demonstrated that the assumption of internal versus external mixing significantly alters bulk optical properties, affecting modeled radiative forcing estimates (Lesins et al., 2002; Chandra et al., 2004). These studies

https://doi.org/10.5194/egusphere-2026-3777
Preprint. Discussion started: 11 August 2026

highlighted the necessity of explicitly incorporating complex mixing states into optical models to achieve closure between modeled and measured optical properties. Subsequent studies advanced both the measurements and modeling frameworks used in optical inversion. Previously, the forward model employed for the optical inversion was the Optical Properties of Aerosols and Clouds (OPAC) model (Hess et al., 1998; Koepke et al., 2015) in conjunction with the core-shell Mie codes (BHCOAT; Bohren and Huffman (1998)). While foundational and widely used, the determination of complex mixing states is limited with OPAC due to the inherent assumption of external mixing and the constraint on the number of components that can be mixed to constitute a mixture. To address this, various studies integrated pre-calculated core-shell optical properties into the OPAC database as user-defined components at the expense of existing ones (Dey et al., 2008; Srivastava et al., 2016). In these studies, the mixing state of aerosols using the OPAC model was modeled by iteratively comparing modeled optical parameters such as the aerosol optical depth (AOD), single scattering albedo (SSA), and the asymmetry parameter (g) with measured ones for different mixing scenarios until the modeled values converge within the measurement errors. Although such an approach enabled the representation of internal mixing within OPAC, both the diversity of mixing scenarios evaluated and the specific aerosol components they comprised were constrained by the model's limited component consideration, and the associated codes remain unavailable to the broader scientific community. The MATLAB code AEROgui (Pedrós et al., 2014) and the Python package AeroMix (Raj et al., 2024) are such tools made available to the scientific community with an explicit option to incorporate internally mixed particles in the calculation of bulk optical properties. Leveraging the capability of AeroMix to model any number of aerosol components in a mixture, Raj et al. (2024) demonstrated that considering all mixing state assumptions simultaneously, rather than examining a limited number of separate scenarios, reveals the likely presence of multiple core-shell mixed aerosol components alongside homogeneous components.

The inferred aerosol mixing states by inverting the optical properties were only deemed as probable mixing states or optically equivalent aerosol mixtures in the previous studies. The heuristic nature of the approach limited the referred studies from the quantification of uncertainties in the inferred mixing states. To address this gap, this study presents an analytical formulation of the optical inversion technique in Sect. 2 that explicitly characterizes its inherently ill-posed and ill-conditioned nature. To address these mathematical challenges, Sect. 3 evaluates the physical feasibility and numerical stability of the inversion framework, establishing the necessity of characterizing the entire feasible solution space. Section 4 reformulates the inversion framework into a system of linear inequalities to construct a geometric, convex polytope representation of the solution space. An empirical evaluation of this geometric confinement is presented in Sect. 5 followed by the recommendations of the study in Sect. 6.

2 Analytical formulation of the optical inversion to model aerosol mixing state

The physical basis of the optical inversion technique lies in Mie theory (Mie, 1908), which provides an exact analytical solution to the scattering and absorption of electromagnetic radiation by homogeneous, isotropic spherical particles. For a particle of radius r and complex refractive index m, Mie theory yields the fundamental optical properties such as the extinction (Q_{ext}), scattering (Q_{sca}), and absorption (Q_{abs}) efficiencies at a specific wavelength λ. The bulk optical coefficients ($\beta_{\mathrm{ext,sca,abs},j}$) for

https://doi.org/10.5194/egusphere-2026-3777
Preprint. Discussion started: 11 August 2026

a polydisperse distribution of the j-th aerosol component can then be calculated by integrating these single-particle properties over the number size distribution $N_j(r)$ from radius $r_{\min}$ to $r_{\max}$ (Eq. 1).

$$\beta_{\text{ext,sca,abs},j}(\lambda) = \int_{r_{\min}}^{r_{\max}} \pi r^2 Q_{\text{ext,sca,abs},j}(m,\lambda,r) N_j(r)\,\mathrm{d}r. \tag{1}$$

Similarly, the total mass concentration M_j of that component is given by integrating the mass of individual particles over the same number size distribution:

$$M_j = \int_{r_{\min}}^{r_{\max}} \frac{4}{3}\pi r^3 \rho_j N_j(r)\,\mathrm{d}r, \tag{2}$$

where ρ_j is the particle density.

Finally, the extinction, scattering, or absorption coefficient per unit mass concentration ($1\,\mu\mathrm{g\,m^{-3}}$) of the j-th component can be written as

$$\overline{\beta_{\text{ext,sca,abs},j}(\lambda)} = \frac{\beta_{\text{ext,sca,abs,j}}(\lambda)}{M_j}. \tag{3}$$

However, many atmospheric aerosol particles, particularly those that have undergone aging processes, are not homogeneous. A crucial extension of the Mie theory is the solution for scattering by a homogeneous sphere of one material coated by a concentric spherical shell of another, known as core-shell Mie theory (Bohren and Huffman, 1998). This calculation requires the complex refractive indices of core (m_c) and shell (m_s) components, as well as their respective radii from the centre (r_c and r_s). The bulk optical properties are then calculated by assuming that the core-shell mixed particles follow the size distribution of the shell component (Arimoto et al., 2006). The core radius r_c for each particle is determined by the core-to-shell radius ratio (CSR), defined as

$$\mathrm{CSR} = \frac{r_c}{r_s} = \left(1 + \frac{M_s \rho_c}{M_c \rho_s}\right)^{-1/3} \tag{4}$$

,where M_c and M_s are the mass contributions of the core and shell components to the mixing, and ρ_c and ρ_s are their respective specific mass densities (Chandra et al., 2004; Srivastava et al., 2016). Consequently, the effective density (ρ_{eff}) of a core-shell mixed component is given by Raj et al. (2024) as

$$\rho_{\text{eff}} = \rho_c \mathrm{CSR}^3 + \rho_s(1 - \mathrm{CSR}^3) \quad . \tag{5}$$

This enables the modelling of optical effects of core-shell mixed aerosols, one of the most important internal mixing configurations prevalent in the atmosphere. The ability to model the optical properties of both homogeneous particles and heterogeneous core-shell particles forms the theoretical basis for the inversion technique.

For an aerosol mixture constituted by n distinct components, the bulk optical properties are modelled assuming the additivity of the optical coefficients of the individual populations. From Eq. (3), the total extinction, scattering or absorption coefficient for the mixture is the linear sum weighted by the total mass concentration M_j of each component (Hess et al., 1998) given as

https://doi.org/10.5194/egusphere-2026-3777
Preprint. Discussion started: 11 August 2026

$$\beta_{\text{ext,sca,abs}}(\lambda) = \sum_{j=1}^{n} M_j \overline{\beta_{\text{ext,sca,abs},j}(\lambda)}. \tag{6}$$

The AOD, which is the vertical integral of β_{ext} in an atmospheric layer bounded by the altitude levels h_{min} and h_{max}, can also be represented as a linear equation as follows

$$\text{AOD}(\lambda) = \sum_{j=1}^{n} M_j \overline{\beta_{\text{ext},j}(\lambda)}(M_j(h_{\text{max}}) - M_j(h_{\text{min}})). \tag{7}$$

A detailed description of the representation of homogeneous and core-shell mixed particles in optical modelling is already provided in Raj et al. (2024) and thus not repeated here.

Referring to Eq. (6) and Eq. (7), the relationship between the aerosol concentrations and the spectral measurements of any of these optical properties or their combinations can be expressed as a system of linear equations of the form $\mathbf{A} \cdot \mathbf{X} = \mathbf{B}$. For a system of n aerosol components and k spectral measurements of aerosol optical properties, $\mathbf{A}$ is the $k \times n$ coefficient matrix that can be computed using a forward optical model such as AeroMix (Raj et al., 2024). $\mathbf{B}$ is the $k \times 1$ observation vector containing the measured spectral optical properties and $\mathbf{X}$ is the $n \times 1$ state vector of unknowns, representing the mass concentrations (M_j) of all probable homogeneous and core-shell components.

A system of n components constrained by p wavelengths of β_{abs} measurements and q wavelengths of β_{sca} measurements where $p + q = k$, can be represented explicitly as

$$\begin{pmatrix} \overline{\beta_{\text{abs},1}(\lambda_{\text{abs},1})} & \overline{\beta_{\text{abs},2}(\lambda_{\text{abs},1})} & \cdots & \overline{\beta_{\text{abs},n}(\lambda_{\text{abs},1})} \\ \overline{\beta_{\text{abs},1}(\lambda_{\text{abs},2})} & \overline{\beta_{\text{abs},2}(\lambda_{\text{abs},2})} & \cdots & \overline{\beta_{\text{abs},n}(\lambda_{\text{abs},2})} \\ \vdots & \vdots & \ddots & \vdots \\ \overline{\beta_{\text{abs},1}(\lambda_{\text{abs},p})} & \overline{\beta_{\text{abs},2}(\lambda_{\text{abs},p})} & \cdots & \overline{\beta_{\text{abs},n}(\lambda_{\text{abs},p})} \\ \overline{\beta_{\text{sca},1}(\lambda_{\text{sca},1})} & \overline{\beta_{\text{sca},2}(\lambda_{\text{sca},1})} & \cdots & \overline{\beta_{\text{sca},n}(\lambda_{\text{sca},1})} \\ \overline{\beta_{\text{sca},1}(\lambda_{\text{sca},2})} & \overline{\beta_{\text{sca},2}(\lambda_{\text{sca},2})} & \cdots & \overline{\beta_{\text{sca},n}(\lambda_{\text{sca},2})} \\ \vdots & \vdots & \ddots & \vdots \\ \overline{\beta_{\text{sca},1}(\lambda_{\text{sca},q})} & \overline{\beta_{\text{sca},2}(\lambda_{\text{sca},q})} & \cdots & \overline{\beta_{\text{sca},n}(\lambda_{\text{sca},q})} \end{pmatrix} \begin{pmatrix} M_1 \\ M_2 \\ \vdots \\ M_n \end{pmatrix} = \begin{pmatrix} \beta_{\text{abs}}(\lambda_{\text{abs},1}) \\ \beta_{\text{abs}}(\lambda_{\text{abs},2}) \\ \vdots \\ \beta_{\text{abs}}(\lambda_{\text{abs},p}) \\ \beta_{\text{sca}}(\lambda_{\text{sca},1}) \\ \beta_{\text{sca}}(\lambda_{\text{sca},2}) \\ \vdots \\ \beta_{\text{sca}}(\lambda_{\text{sca},q}) \end{pmatrix}. \tag{8}$$

Any bulk optical property, such as β_{ext} or AOD, which is a linear sum of the coefficients of individual components, can be incorporated in this system to further constrain $\mathbf{X}$. However, AOD is excluded from the inversion framework in this study due to its high sensitivity to uncertainties in aerosol vertical distribution (Sinha et al., 2013; Raj et al., 2024). Parameters such as SSA and g can not be considered, as they do not scale linearly with component concentrations. Nevertheless, the constraining effect of SSA and AOD are inherently preserved since both β_{abs} and β_{sca} are already incorporated into the system.

https://doi.org/10.5194/egusphere-2026-3777
Preprint. Discussion started: 11 August 2026

2.1 Determination of aerosol composition and mixing state

Each element of $\mathbf{X}$ represents the respective mass concentrations of each aerosol component under consideration. To accurately capture the true composition and mixing state of an aerosol mixture, the formulation must initially consider a comprehensive set of all probable components to test for their presence in the mixture. This set must include not only homogeneous aerosol components but also every plausible core-shell configuration defined at discrete CSRs (Raj et al., 2024). Each of these homogeneous and core-shell components is treated mathematically as a distinct component, assuming no physical or chemical interactions between the particles. If a specific aerosol component or a core-shell mixed state is not considered in the set of probable components and thus not present in the coefficient matrix $\mathbf{A}$, the algorithm fundamentally cannot retrieve its presence, regardless of whether it actually exists in the mixture.

When solved for $\mathbf{X}$, this linear system will yield the specific mass concentrations of the aerosol components in the mixture required to reproduce the measured optical properties. Since $\mathbf{X}$ is intentionally constructed to encompass all probable components to assess their existence, a real atmospheric aerosol mixture will typically contain only a small subset of them. Consequently, the true solution vector $\mathbf{X_{true}}$ will be inherently sparse: the components present in the mixture will resolve to non-zero positive values, while non-existent components will evaluate to zero.

Once $\mathbf{X}$ is resolved, the mixing state of the aerosol population can be quantitatively inferred by analyzing the mass distribution across the components (Raj et al., 2024). The total mass distributed among the homogeneous components constitutes the externally mixed aerosol mass fraction, while the mass distributed among the core-shell mixed aerosols constitutes the internally mixed aerosol mass fraction. A population is determined to be $100\,\%$ externally mixed if the total retrieved aerosol mass is distributed exclusively among the homogeneous components. Conversely, a mixture in which the mass is distributed exclusively among core-shell mixed aerosols represents a $100\,\%$ internally mixed state. The absolute masses of core and shell fractions within a core-shell mixed structure are decoupled and computed using the CSR and their respective particle densities (Eq. 4). The combined mass of an aerosol component distributed across various core–shell mixed particles and its purely externally mixed state (homogeneous) contributes to the total mass of that aerosol component in the mixture. Since the mixing state is directly computed from the distribution of aerosol mass among different components, the state vector $\mathbf{X}$ inherently defines the aerosol mixing state. For this reason, the terms “aerosol component concentrations” and “aerosol mixing state” are used interchangeably throughout this study when referring to $\mathbf{X}$ or its solution space.

2.2 Advantages of analytical formulation over heuristic approaches

Formulating the optical inversion problem as a linear system $\mathbf{A} \cdot \mathbf{X} = \mathbf{B}$ offers distinct advantages over the heuristic, iterative “best-fit” approaches traditionally employed in aerosol closure studies. First, the method is inherently scalable. Unlike iterative search algorithms, which suffer from computational bottlenecks as the dimensionality of the search space increases, the linear algebraic formulation can efficiently handle an arbitrary number of aerosol components (n) and spectral measurements of aerosol optical properties (k). This allows for the inclusion of all possible mixing state assumptions for a realistic representation and any number of linearly independent measurements to reduce uncertainty in the inferred mixing state.

https://doi.org/10.5194/egusphere-2026-3777
Preprint. Discussion started: 11 August 2026

Second, the framework is modular, remaining agnostic to the specific forward models or instruments. The coefficient matrix $\mathbf{A}$ serves as a representation of component-wise spectral optical properties; which can be constructed using any optical model (e.g., AeroMix, AERObui, OPAC, T-matrix codes (Waterman, 1971; Mishchenko et al., 1999)) without altering the linear framework. Similarly, the observation vector $\mathbf{B}$ is independent of the specific instrument measuring aerosol spectral optical properties (e.g., light-scattering photometers, filter-based absorption photometers, and Sunphotometers). While the accuracy of the final solution naturally depends on the fidelity of the inputs, as the accuracy of the forward model representations ($\mathbf{A}$) improves with better aerosol size distribution and refractive index data, the inversion results will systematically become more accurate without requiring changes to the algorithm itself.

2.3 Challenges in the optical inversion framework

While the linear formulation provides a robust mathematical framework, explicitly defining the optical inversion as an algebraic system exposes fundamental mathematical challenges that are effectively invisible within heuristic methods. Consequently, applying this framework to real-world aerosol data introduces significant challenges related to the system's mathematical properties, as outlined below.

2.3.1 Ill-posed nature of the optical inversion framework

To accurately characterize the complexity of atmospheric aerosols, the model must consider a comprehensive set of physically feasible homogeneous and core-shell components. Consequently, the number of potential components (n) frequently exceeds the number of possible spectral optical measurements (k), rendering the system strictly underdetermined ($k < n$) and ill-posed.

In linear algebra, a strictly underdetermined system $\mathbf{A} \cdot \mathbf{X} = \mathbf{B}$ does not yield a unique solution; rather, it allows for an infinite solution space. Mathematically, the general solution can be expressed as $\mathbf{X} = \mathbf{X}_p + \mathcal{N}(\mathbf{A})\alpha$ where $\mathbf{X}_p$ is a particular solution satisfying the equation $\mathbf{A} \cdot \mathbf{X}_p = \mathbf{B}$, $\mathcal{N}(\mathbf{A})$ is a matrix whose columns form a basis of the null space of $\mathbf{A}$, and α is a vector of free parameters. The dimension of α corresponds to the nullity of $\mathbf{A}$, which is defined as $n - \mathrm{rank}(\mathbf{A})$. For a full-rank system, this nullity is $n - k$, dictating that the $n - k$ degrees of freedom within α control a continuous space of mathematically valid solutions, rather than yielding a single unique solution.

This formulation explicitly demonstrates that there exists a set of valid concentration vectors—parameterized by α—that produce identical optical signatures. This implies that multiple distinct mixing states can be optically equivalent, making the deterministic inference of a single "true" mixing state impossible without probabilistic characterization or additional constraints.

2.3.2 Ill-conditioned nature of the optical inversion problem

A second critical challenge arises from the inherent uncertainties in the measurement of aerosol spectral optical properties. The observation vector $\mathbf{B}$ is never exact; it is always accompanied by measurement uncertainty $\boldsymbol{\epsilon}$, such that $\mathbf{B}_{measured} = \mathbf{B}_{true} \pm \boldsymbol{\epsilon}$. If the coefficient matrix $\mathbf{A}$ is ill-conditioned, small perturbations in $\mathbf{B}$ can lead to disproportionately large fluctuations in the

https://doi.org/10.5194/egusphere-2026-3777
Preprint. Discussion started: 11 August 2026

solution vector $\mathbf{X}$. Mathematically, the sensitivity of a linear system is quantified by the matrix's condition number (Strang, 1980). For a rectangular matrix $\mathbf{A}$, the condition number $c(\mathbf{A})$ is defined as the product of the norm of the matrix and the norm of its pseudoinverse ($\mathbf{A}^+$) (Eq. 9).

$$c(\mathbf{A}) = \|\mathbf{A}\|\|\mathbf{A}^+\|. \tag{9}$$

The condition number acts as a multiplier for uncertainty. The relationship between the relative error in the spectral observations ($\frac{\|\Delta\mathbf{B}\|}{\|\mathbf{B}\|}$) and the theoretical maximum relative error in the inferred aerosol component concentrations ($\frac{\|\Delta\mathbf{X}\|}{\|\mathbf{X}\|}$), which translates to mixing states, is strictly bounded by the inequality,

$$\frac{\|\Delta\mathbf{X}\|}{\|\mathbf{X}\|} \leq c(\mathbf{A})\frac{\|\Delta\mathbf{B}\|}{\|\mathbf{B}\|}. \tag{10}$$

In the context of aerosol optical inversion, this ill-conditioning arises from two primary physical factors. First, many aerosol components exhibit highly correlated or spectrally similar absorption and scattering signatures, resulting in near-linear dependence among the columns of $\mathbf{A}$. This is discussed in detail in section 3.2. Second, the optical efficiencies of different species can vary by orders of magnitude (e.g., strong absorbers like black carbon versus scattering-dominant sulfates). This implies that direct inversion methods risk amplifying the measurement noise in $\mathbf{B}$ by a factor of up to $c(\mathbf{A})$, leading to disproportionately large errors in the estimated state vector $\mathbf{X}$.

3 Physical feasibility and optical distinguishability of aerosol components

To illustrate the aerosol optical inversion problem, an initial set of 85 probable components is considered, including five homogeneous aerosol types: water-insoluble (IS), water-soluble (WS), black carbon (BC), accumulation mode of sea-salt (SS), nucleation mode of mineral dust (MD); and their 80 possible core-shell combinations at various CSR values ranging from 0.2 to 0.8 with an increment of 0.2. An overview of the various parameters that describes the homogeneous aerosol types is given in Table 1. This section evaluates the feasibility of resolving this system by addressing its ill-posed and ill-conditioned nature. To achieve this, it aims to reduce the dimensionality and quantify the uncertainty of the inversion model by establishing the physical feasibility of various core-shell combinations, characterizing the spectral distinguishability of the components, and imposing strict physical boundaries on the calculated aerosol component concentrations to ensure inferred aerosol mixing states remain physically realistic.

3.1 Identification of physically feasible core-shell aerosol combinations

The formation of core-shell mixed aerosols is driven by specific processes such as the condensation of volatile species (Li et al., 2016), coagulation (Arimoto et al., 2006), and cloud processing (Andreae et al., 1986). Consequently, only a specific subset of core-shell permutations physically exists in the atmosphere. Observational evidence indicates that WS species (e.g., ammonium, sulfates, nitrates) typically form coatings on other particles rather than acting as cores for other primary aerosols. Similarly, MD, being large and irregular, is unlikely to form a uniform coating over other aerosols like IS, WS, BC or SS.

https://doi.org/10.5194/egusphere-2026-3777
Preprint. Discussion started: 11 August 2026

Table 1. Size distribution parameters, specific densities, and refractive indices of predefined aerosol components in the dry state (RH = 0%) (Koepke et al., 1997; Hess et al., 1998; Raj et al., 2024).

Aerosol component	**Constituting species**	**Mode radius** [µm]	**Geometric standard deviation**	**Specific density** [$\mathrm{g\,cm^{-3}}$]	**Refractive index at 0.5µm**
Insoluble (IS)	Soil dust, fly ash, and non-hygroscopic organic matter	0.471	2.51	2.0	$1.53 + 8 \times 10^{-3} i$
Water-soluble (WS)	SO_4^{2-}, NO_3^-, NH_4^+, and hygroscopic fraction of organic matter	0.0212	2.24	1.8	$1.53 + 5 \times 10^{-3} i$
Black carbon (BC)	Black carbon aerosols	0.0118	2	1.8	$1.75 + 4.5 \times 10^{-1} i$
Sea-salt accumulation mode (SS)	Sea-salt aerosols	0.209	2.03	2.2	$1.5 + 1.55 \times 10^{-8} i$
Mineral dust nucleation mode (MD)	Desert dust	0.007	1.95	2.6	$1.53 + 7.8 \times 10^{-3} i$

Based on the observational evidence summarized in Table 2, physically infeasible combinations, such as those with WS cores or MD shells, can be excluded from the set of probable core-shell mixed components. This will reduce the dimensionality of the problem without compromising on the assumptions of probable mixing states. It is also crucial to note that assuming a perfect concentric core-shell configuration often deviates from reality. Actual internally mixed aerosol morphologies span a complex continuum, ranging from concentric spheres to eccentric cores, partially engulfed inclusions, and fractal aggregates (Andreae et al., 1986; Scarnato et al., 2013; Li et al., 2016). To address this, future modeling frameworks must progress from simplified concentric core-shell approximations by integrating advanced scattering codes—specifically, by implementing the Discrete Dipole Approximation (DDA) (Draine and Flatau, 1994) to resolve arbitrary geometries.

3.2 Identification of optically similar aerosol components

The numerical stability of the linear system $\mathbf{A} \cdot \mathbf{X} = \mathbf{B}$ is critically dependent on the orthogonality of the column vectors in the coefficient matrix $\mathbf{A}$. After excluding physically infeasible core-shell combinations from the initial set of probable components, the reduced set has 57 probable components. If this system is to be constrained with 13 measurements (β_{sca} at four bands from 0.45 to 0.6 µm and β_{abs} at nine bands from 0.4 to 0.9 µm), the condition number for this formulated coefficient matrix $\mathbf{A}$ is determined to be $c(A) \approx 10^{4.52}$. According to Eq. (10), a condition number of this magnitude dictates that any fractional measurement uncertainty in the optical properties can theoretically be amplified by a factor of $c(\mathbf{A})$ in the resulting concentration vector $\mathbf{X}$.

https://doi.org/10.5194/egusphere-2026-3777
Preprint. Discussion started: 11 August 2026

Table 2. Summary of observed Core-Shell aerosol configurations.

Core	Shell	Study location/type	Reference
IS/Fly ash	WS	Mt. Tai, China	Li et al. (2016)
		Asian dust over Japan	Kojima et al. (2006)
BC	IS	Laboratory experiment	Dalirian et al. (2018)
	WS	Xi'an, China	Dong et al. (2019)
		New Delhi, India	Mishra et al. (2018)
		Asian dust over Japan	Kojima et al. (2006)
	SS	Laboratory experiment	Scarnato et al. (2013)
SS	IS (Organic matter)	Atlantic marine air	O'Dowd et al. (2004)
	WS (Organic matter)	Laboratory experiment	Hu et al. (2024); Song et al. (2024)
		Macao, China	Li et al. (2011)
		Asian dust over Japan	Kojima et al. (2006)
	BC	Laboratory experiment	Scarnato et al. (2013)
MD	IS	Laboratory experiment	Wang et al. (2018)
	WS	Asian dust over Japan	Kojima et al. (2006)
		Beijing, China	Li and Shao (2009)
		Xianghe, China	Li et al. (2016)
	BC	Asian dust over Yellow Sea	Arimoto et al. (2006)
	SS	Equitorial Pacific Ocean	Andreae et al. (1986)

This highly elevated condition number indicates that the matrix $\mathbf{A}$ is severely ill-conditioned, which is primarily a result of spectral collinearity among the aerosol components under consideration. In other words, the optical signatures of these various homogeneous and core-shell aerosol components lack sufficient spectral orthogonality to be uniquely resolved. To assess the collinearity and explicitly identify the spectrally similar components, a hierarchical cluster analysis is performed using the normalized root mean square error (NRMSE) as a pairwise distance metric. For any pair of aerosol components i and j, the pairwise NRMSE is calculated as

$$\mathrm{NRMSE}_{i,j} = \frac{\sqrt{\frac{1}{k}\sum_{m=1}^{k}\left(y_{i,m} - y_{j,m}\right)^2}}{\max(y_{i,m}, y_{j,m}) - \min(y_{i,m}, y_{j,m})}, \tag{11}$$

https://doi.org/10.5194/egusphere-2026-3777
Preprint. Discussion started: 11 August 2026

where k represents the total number of wavelengths considered in the spectral measurements of aerosol optical properties ($k = p + q$) and y_i and y_j are the arrays comprising combined spectral scattering and absorption coefficients across the wavelength range of 0.25 to 1 μm of the paired aerosol components. NRMSE was selected over correlation or Euclidean distances because it estimates the spectral differences relative to the scale of the component pair. While correlation distance effectively captures similarities in spectral shape, it neglects differences in absolute magnitude, potentially grouping strong absorbers with weak absorbers that exhibit similar spectral slopes. Conversely, Euclidean distance is heavily biased toward components with large optical efficiencies, often failing to distinguish between weak signals.

The critical threshold for similarity, below which a component pair is deemed optically indistinguishable from each other, is proposed to be strictly dictated by the uncertainties associated with the measurements. If the theoretical difference between the optical spectra of a given pair falls within the measurement uncertainty, they cannot be resolved by the inversion. To demonstrate this hierarchical clustering within the current framework, an arbitrary measurement uncertainty of 5% is considered, establishing a nominal similarity threshold of 95% ($\mathrm{NRMSE} \leq 0.05$) to identify groups of components that are indistinguishable to the optical inversion algorithm. In practical applications, the similarity threshold must be selected to reflect the exact uncertainties associated with the measurement techniques employed and other relevant factors.

Figure 1 is a clustergram showing the pairwise NRMSE heatmap of aerosol components in conjunction with a dendrogram hierarchically clustering the optically similar pairs. Each core-shell mixed component in this figure is labeled in the format core_shell_CSR. The NRMSE range of the heatmap represents the degree of optical similarity, with zero indicating high similarity and one indicating significant spectral divergence. A red dashed line is placed at the $\mathrm{NRMSE} \leq 0.05$ threshold, identifying groups that are at least 95% similar. Components clustered below this line are considered optically indistinguishable for the purposes of the inversion, effectively limiting the resolution of the inversion process. The analysis reveals that the optical properties of core-shell mixed aerosol particles are more similar to their shell component than their core component. The thickly coated (CSRs of 0.2) core-shell components were found to be optically indistinguishable from the pure form of their shell component within 5% uncertainty. For WS-coated aerosols, except for those with BC cores, even the thinly coated (CSRs of 0.6 to 0.8) components are more than 95% optically similar to pure WS. For core-shell components thinly coated with BC, the particles become distinguishable from pure BC. However, within each CSR group, they are indistinguishable from each other; in other words, an IS, SS, or MD aerosol particle coated with the same thin layer of BC will appear optically identical.

This high degree of optical similarity among various components implies that the thickly coated core-shell mixed states are optically indistinguishable from their shell component in pure form within the 5% measurement uncertainty. The presence of optically indistinguishable components inflates the condition number of matrix $\mathbf{A}$, thereby amplifying the sensitivity of the inferred concentrations to measurement uncertainties. While optically similar components can be grouped into reduced "optical classes" to improve the stability, the inherent non-uniqueness caused by the spectral collinearity implies that standard optimization techniques, which yield a single deterministic best-fit solution, are not a suitable approach to this problem. Rather, techniques to characterize the entire feasible solution space must be employed to determine all probable mixing states.

https://doi.org/10.5194/egusphere-2026-3777
Preprint. Discussion started: 11 August 2026

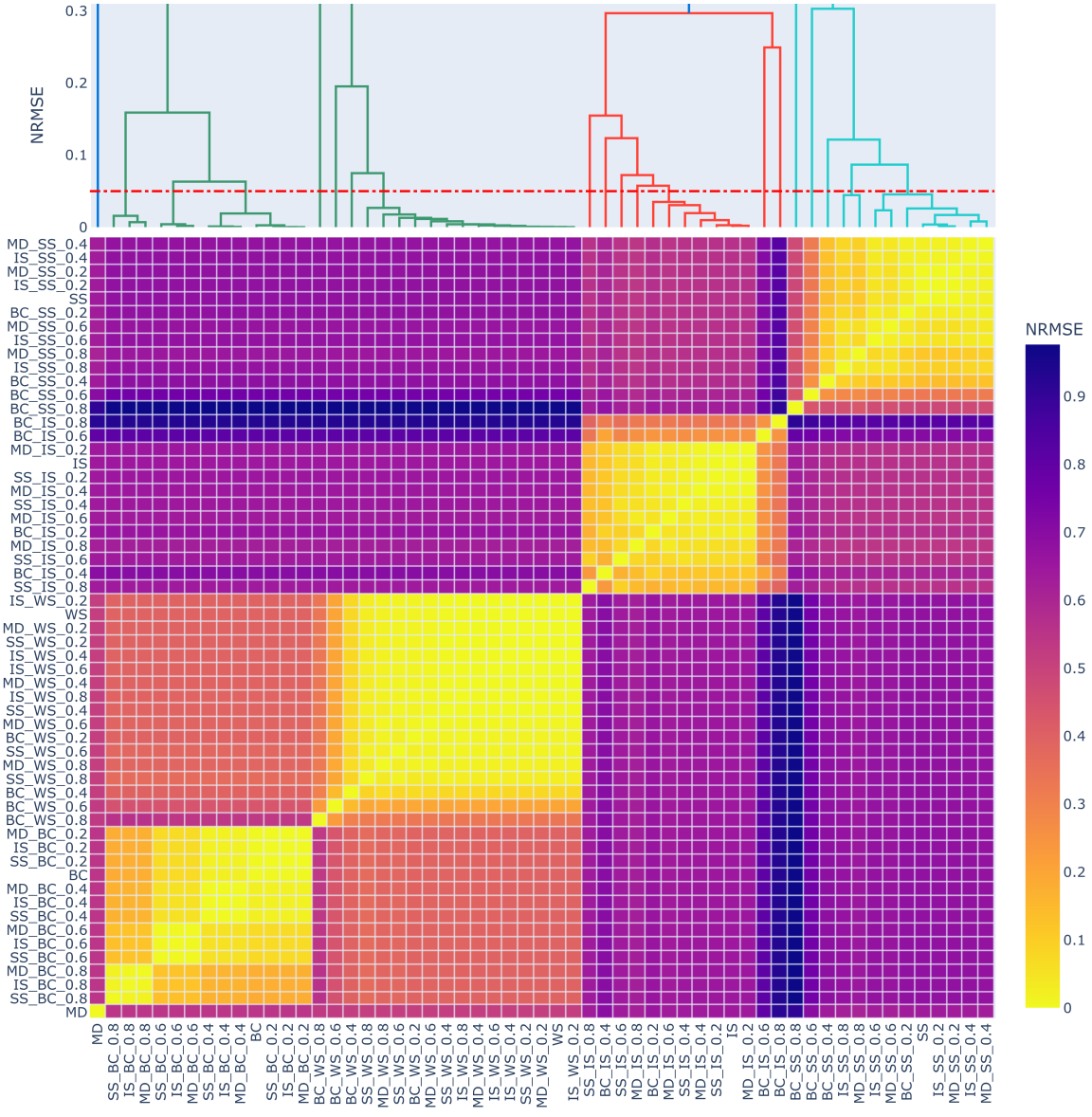

Figure 1. Clustergram illustrating the normalized root mean square error (NRMSE) between each paired component and hierarchical clusters depicting the component clusters that are similar for different NRMSE values. The red dashed line corresponds to NRMSE=0.05, which is the threshold for 95% similarity between aerosol components.

https://doi.org/10.5194/egusphere-2026-3777
Preprint. Discussion started: 11 August 2026

3.3 Physical constraints on aerosol component concentrations

While reducing the number of unknowns addresses the matrix conditioning, the ill-posed nature of the problem implies that an infinite set of solutions may still satisfy the linear system $\mathbf{A} \cdot \mathbf{X} = \mathbf{B}$ within measurement error. To restrict these mathematically valid solutions to a physically meaningful range, physical boundaries must be applied to the unknown concentrations in $\mathbf{X}$. First, a non-negativity constraint ($\mathbf{X} \geq 0$) is strictly imposed, as aerosol mass concentrations cannot be negative. Second, a maximum concentration limit ($\mathbf{X} \leq \mathbf{X}_{\max}$) must be established, derived either from total measured aerosol mass concentrations or from regional climatological averages. By imposing these strict lower and upper limits, the potentially infinite range of mathematically equivalent concentrations is confined to a strictly finite region. This ensures that all inferred mixing states remain physically realistic.

4 Characterization of the solution space of aerosol mixing states

The inherent ill-posed and ill-conditioned nature of the aerosol optical inversion problem renders the search for a single, unique aerosol mixing state effectively impossible. Since the number of potential aerosol components (n) often exceeds the number of independent spectral optical measurements (k), and measurement data always contains uncertainty, multiple distinct mixing states can produce identical optical signatures. Consequently, deterministic methods that seek a single "best-fit" solution are mathematically unstable and are not guaranteed to retrieve the true mixing state but a probable one only. To address this challenge, this study proposes to reformulate the optical inversion problem from seeking an optimal probable solution into a characterization of the entire feasible solution space of probable mixing states.

Instead of forcing the model to match the observations exactly ($\mathbf{A} \cdot \mathbf{X} = \mathbf{B}$), the problem is defined as finding all probable solutions $\mathbf{X}$ that reproduce the observations within the measurement uncertainty ($\boldsymbol{\epsilon}$). This transforms the system into a set of linear inequalities as follows

$$\mathbf{B} - \boldsymbol{\epsilon} \leq \mathbf{A} \cdot \mathbf{X} \leq \mathbf{B} + \boldsymbol{\epsilon}. \tag{12}$$

Geometrically, each k-th row of this system defines a region in the high-dimensional solution space located between a pair of parallel hyperplanes, $\mathbf{A}_k \cdot \mathbf{X} \leq \mathbf{B}_k + \boldsymbol{\epsilon}_k$ and $\mathbf{A}_k \cdot \mathbf{X} \geq \mathbf{B}_k - \boldsymbol{\epsilon}_k$. The intersection of these multiple half-spaces forms the solution space, within which every point is mathematically consistent with the measured aerosol optical properties.

To ensure the solutions are physically meaningful, this unbounded region is further constrained by geometric bounds established in Sect. 3.3. The non-negativity constraint restricts solutions to the half-space defined by $-\mathbf{X} \leq 0$, while the upper bound restricts them to $\mathbf{X} \leq \mathbf{X}_{\max}$.

The final feasible solution space is defined as the intersection of all these half-spaces: the measurement-defined regions, the non-negativity half-spaces, and the upper-bound half-spaces. The intersection of a finite number of half-spaces forms a convex polytope. The set of all points within this polytope represents all mixing states that are both physically possible and consistent with the measured aerosol spectral optical properties. The half-representation (H-space representation) of this polytope can be

https://doi.org/10.5194/egusphere-2026-3777
Preprint. Discussion started: 11 August 2026

expressed as

$$\begin{bmatrix} \mathbf{A} \\ -\mathbf{A} \\ \mathbf{I} \\ -\mathbf{I} \end{bmatrix} \mathbf{X} \leq \begin{bmatrix} \mathbf{B}+\boldsymbol{\epsilon} \\ -\mathbf{B}+\boldsymbol{\epsilon} \\ \mathbf{X}_{\max} \\ 0 \end{bmatrix}, \tag{13}$$

where $\mathbf{I}$ is the identity matrix of order n. This matrix formulation defines the boundaries of the solution space, where every point contained within the polytope is a valid solution to the optical inversion problem.

While preserving the scalability and model-agnostic advantages of the initial linear framework as explained in Sect. 2.2, the reformulated framework (Eq. 13) addresses the non-uniqueness of the solution caused by ill-posedness and large solution uncertainties caused by ill-conditioning. By explicitly incorporating the uncertainty in optical measurements $\boldsymbol{\epsilon}$, the framework allows for the characterization of all the possible solutions, rather than seeking a single deterministic solution that is susceptible to measurement errors.

Although every point within this convex polytope is a mathematically valid solution, not all are equally probable in the atmosphere. Of the n probable components considered in this optical inversion problem to test for their existence, atmospheric aerosol mixtures typically contain only a subset. Consequently, the solution vector $\mathbf{X}$ is highly likely to be sparse, meaning a significant number of its components are exactly zero. Although the sparsest solution is not guaranteed to be the true state, the true state is almost certainly not a mixture containing all the assumed components. Mathematically, even if the solution is not strictly sparse, the presence of just a single zero-concentration component in $\mathbf{X}$ fundamentally constrains its location within the polytope. Consider any solution vector $\mathbf{X} \in P$, where $P \subseteq \mathbb{R}^n$ is the convex polytope defined by the system of linear inequalities as shown in Eq.13. Let this system be expressed in the generalized matrix form

$$\mathbf{G} \cdot \mathbf{X} \leq \mathbf{h}, \tag{14}$$

where each row k represents a single linear constraint $g_k \cdot X \leq h_k$. The definition of the strict interior of the polytope, denoted as $\text{int}(P)$, requires that a point $\mathbf{X}$ strictly satisfy all defining inequalities

$$\mathbf{X} \in \text{int}(P) \iff g_k \cdot \mathbf{X} < h_k \quad \forall k. \tag{15}$$

One subset of these constraints is the physical non-negativity requirement for each component j, represented as $-M_j \leq 0$ (or $M_j \geq 0$). For a point to be in the strict interior, the concentration of every component must be strictly positive ($M_j > 0$).

If a solution $\mathbf{X}$ is sparse, there exists at least one component j such that its concentration is zero ($M_j = 0$). This condition satisfies the non-negativity constraint as an equality.

$$M_j = 0 \implies -M_j = 0. \tag{16}$$

Since the condition for the strict interior ($M_j > 0$) is violated, the sparse solution $\mathbf{X}$ cannot lie in the interior of P ($\mathbf{X} \notin \text{int}(P)$). Geometrically, the set of points where at least one linear inequality holds as an equality defines a facet of the polytope.

https://doi.org/10.5194/egusphere-2026-3777
Preprint. Discussion started: 11 August 2026

Therefore, any solution $\mathbf{X}$ where at least one component is zero must lie on the boundary of P, specifically on the facets defined by the coordinate hyperplanes ($M_j = 0$). This insight significantly reduces the search for physically probable solutions from the entire volume of P to its lower-dimensional boundaries lying on the coordinate hyperplanes.

5 Evaluation of the analytical formulation using simulated aerosol mixtures

To evaluate the proposed formulation that all physically valid, aerosol mixtures are strictly contained on the boundary of the defined polytope (Eq. 13), the exact component-wise mass concentrations of all homogeneous and core-shell mixed aerosols present within the sampled volume must be known to form a true state vector ($\mathbf{X}_{true}$). Since current observational techniques cannot resolve the exact mass concentration of individual homogeneous and core-shell components within an aerosol mixture, this evaluation utilizes synthetic aerosol mixtures in which $\mathbf{X}_{true}$ is known and their corresponding spectral optical properties modeled with AeroMix. The modeling of optical properties for various aerosol scenarios using AeroMix has been benchmarked against the widely accepted aerosol optical model OPAC (Raj et al., 2024). To generate these mixtures, a system comprising 13 core-shell mixed aerosols with a CSR=0.8 and their five homogeneous counterparts, namely the IS, WS, BC, SS and MD was considered. The core-shell combinations included an IS core with WS, BC, or SS shells; a BC core with IS, WS, or SS shells; an SS core with IS, WS, or BC shells; and an MD core with IS, WS, BC, or SS shells. This configuration yielded an 18-dimensional state space consisting of both homogeneous and core-shell mixed aerosols. Since the framework is scalable, the geometric confinement tested by this evaluation remains valid regardless of the number of probable aerosol components considered in the mixture. A dataset of 10,000 unique aerosol mixtures was generated by randomly selecting the active components and assigning their respective mass concentrations, representing the true state vectors ($\mathbf{X}_{true}$).

The exact optical spectra ($\mathbf{B}_{true}$) corresponding to each $\mathbf{X}_{true}$ were calculated using the AeroMix model. To simulate commonly used instrument measurements, β_{sca} were modeled at 0.45, 0.5, 0.55, and 0.6 µm, and β_{abs} at 0.4, 0.45, 0.5, 0.55, 0.6, 0.65, 0.7, 0.8, and 0.9 µm. These specific wavelengths were chosen as they are supported by the AeroMix model and fall within the widely measured spectral ranges of typical light-scattering photometers (0.45 to 0.635 µm) and filter-based absorption photometers (0.37 to 0.95 µm). To account for measurement error, synthetic noise was applied to the exact optical spectra. A relative measurement uncertainty of 5% was arbitrarily introduced for both scattering and absorption coefficients. The observation vector $\mathbf{B}$ was generated by uniformly sampling each element from the interval $[\mathbf{B}_{true}/(1+\epsilon), \mathbf{B}_{true}/(1-\epsilon)]$ where $\epsilon = 0.05$ represents the 5% relative measurement uncertainty. Subsequently, the absolute measurement uncertainty vector ($\boldsymbol{\epsilon}$) was explicitly defined as 5% of the simulated observation ($\boldsymbol{\epsilon} = 0.05\mathbf{B}$). Additionally, the maximum mass concentration limit, $\mathbf{X}_{\max}$, was dynamically calculated for each case, set to the total mass concentration of the true state plus an additional 10% error margin ($\mathbf{X}_{\max} = 1.1 \sum \mathbf{X}_{true}$). This approach provides a realistic scenario of spectral optical and mass concentration bounds, allowing for an accurate evaluation of whether the polytope boundaries contain the true state despite the measurement uncertainties.

To evaluate whether the true solution ($\mathbf{X}_{true}$) lies within the polytope $\mathbf{G} \cdot \mathbf{X} \leq \mathbf{h}$, $\mathbf{G}$ and $\mathbf{h}$ were constructed as detailed in Sec. 4 and calculated the slack vector ($\boldsymbol{s}$) for every case as $\boldsymbol{s} = \mathbf{h} - \mathbf{G} \cdot \mathbf{X}_{true}$. The elements of $\boldsymbol{s}$ represent the shortest

https://doi.org/10.5194/egusphere-2026-3777
Preprint. Discussion started: 11 August 2026

distances from $\mathbf{X}_{true}$ to every bounding hyperplane of the polytope. A solution is mathematically proven to be contained within the polytope if and only if all elements of its slack vector are non-negative ($\boldsymbol{s} \geq 0$) and is on the boundary if at least one element of the slack vector equals zero ($\min(\boldsymbol{s}) = 0$).

Upon evaluating the 10,000 simulated cases, 100% of the cases yielded a strictly non-negative slack vector, explicitly confirming that the true solution always lies within the formulated polytope. Of the 10,000 simulated mixtures, 28 contained non-zero concentrations for all 18 components. For these cases, the minimum value of $\boldsymbol{s}$ was strictly greater than zero, confirming that these solutions reside within the interior of the polytope and not at the boundary. For the remaining 9,972 cases, which lacked at least one of the 18 active components, the minimum value of $\boldsymbol{s}$ was exactly zero. This empirically proves that any solution containing at least one zero-concentration component is structurally confined to the boundary facets of the polytope.

6 Summary and recommendations

Improved estimates of the direct and indirect effects of aerosols necessitate accurate determination of aerosol mixing states. However, the determination of aerosol mixing states mostly relies on optical inversion techniques owing to a lack of comprehensive direct measurements of aerosol mixing states. This study presents a transition in the optical inversion modeling of aerosol mixing states from heuristic approaches to an analytical framework formulated as a system of linear equalities ($\mathbf{A} \cdot \mathbf{X} = \mathbf{B}$). A distinct advantage of this formulation is its inherent scalability and agnosticism toward both the forward model and the measurements. The framework allows the coefficient matrix ($\mathbf{A}$) to be dynamically constructed for any number of aerosol components with any suitable forward model, such as AeroMix, which can simulate the optical properties of externally mixed and core-shell mixed aerosols. Concurrently, the observation vector ($\mathbf{B}$) can integrate data from diverse measurements of aerosol spectral optical properties. Consequently, the accuracy of the final solution can systematically improve with better aerosol size distribution and refractive index data as well as with more realistic mixing state assumptions.

However, the explicit formulation of the inversion as an algebraic system revealed mathematical challenges that had remained hidden within heuristic techniques. To evaluate the feasibility of solving this deterministic system ($\mathbf{A} \cdot \mathbf{X} = \mathbf{B}$), this study assessed its inherently ill-posed and ill-conditioned nature. Physically infeasible core-shell combinations were excluded based on extensive observational evidence to reduce the system's dimensionality, and the uncertainty associated with the estimation of a deterministic solution was quantified. Using an NRMSE-based hierarchical clustering analysis, spectral collinearity among aerosol components was characterized. These findings demonstrate that direct deterministic inversion methods inevitably amplify instrumental noise and yield erroneous solutions, thereby establishing the necessity of characterizing the entire feasible solution space.

Recognizing these limitations, rather than seeking a single, noise-sensitive deterministic solution, the framework is reformulated as a system of linear inequalities ($\mathbf{B} - \boldsymbol{\epsilon} \leq \mathbf{A} \cdot \mathbf{X} \leq \mathbf{B} + \boldsymbol{\epsilon}$) by incorporating measurement uncertainties ($\boldsymbol{\epsilon}$) and mass concentration bounds ($\mathbf{X} \geq 0$ and $\mathbf{X} \leq \mathbf{X}_{\max}$). Geometrically, this restricts the feasible solution space to a finite convex polytope, within which every point represents a mathematically valid mixing state consistent with the observed optical proper-

https://doi.org/10.5194/egusphere-2026-3777
Preprint. Discussion started: 11 August 2026

ties. Maintaining the scalability and model-agnostic advantages of the initial linear equality framework, this inequality-based approach directly addresses the non-uniqueness caused by ill-posedness and the large uncertainties associated with matrix ill-conditioning. This approach enables the mapping of the entire physically feasible solution space, allowing a probabilistic characterization of aerosol mixing states.

Since atmospheric aerosol mixtures typically contain only a subset of all possible components considered in $\mathbf{X}$, the true solution is highly likely to be sparse. By incorporating this sparsity assumption, the solution region is further constrained to the boundary facets (coordinate hyperplanes) of the solution space. This geometric confinement was empirically demonstrated using 10 000 synthetic aerosol mixtures, revealing that all physically valid solutions fall strictly on the polytope boundaries.

To advance the operational applicability of the proposed analytical formulation for the optical inversion of aerosol mixing state, future work should focus on providing probabilistic inference of the likely mixing state from all mathematically valid mixing states sampled from the solution space. To achieve this, random walk algorithms, such as Markov Chain Monte Carlo (MCMC) methods, can be employed to efficiently sample the high-dimensional boundary space. While this study utilized concentric core-shell approximations, the linear algebraic framework is entirely independent of the forward model. Incorporation of complex particle morphologies such as eccentric cores, partially engulfed inclusions, and fractal aggregates using advanced scattering codes will improve the mixing state estimates using this same framework.

Building on these recommendations, future work will focus on the development and computational implementation of an MCMC-based algorithm within the AeroMix package. This approach will enable the effective exploration of the solution space, transforming optical inversion into a probabilistic determination of aerosol mixing states for their improved representation in radiative transfer models.

Code and data availability. The AeroMix package is publicly available on Zenodo (https://doi.org/10.5281/zenodo.10552079) under GNU General Public License-3.0 (P Raj and Sinha, 2024). The computational codes and data used to perform the analysis presented are available at https://doi.org/10.5281/zenodo.21798191 (P Raj and Sinha, 2026).

Author contributions. PRS conceived the ideas and designed the study. SPR developed the theoretical formalism, performed the analysis, and prepared the original draft with inputs from PRS.

Competing interests. The contact author has declared that none of the authors has any competing interests.

Acknowledgements. The authors gratefully acknowledge IIST for providing the computational facilities.

https://doi.org/10.5194/egusphere-2026-3777
Preprint. Discussion started: 11 August 2026

References

Andreae, M. O., Charlson, R. J., Bruynseels, F., Storms, H., Van Grieken, R., and Maenhaut, W.: Internal Mixture of Sea Salt, Silicates, and Excess Sulfate in Marine Aerosols, Science, 232, 1620–1623, https://doi.org/10.1126/science.232.4758.1620, 1986.

Arimoto, R., Kim, Y., Kim, Y., Quinn, P., Bates, T., Anderson, T., Gong, S., Uno, I., Chin, M., Huebert, B., Clarke, A., Shinozuka, Y., Weber, R., Anderson, J., Guazzotti, S., Sullivan, R., Sodeman, D., Prather, K., and Sokolik, I.: Characterization of Asian Dust during ACE-Asia, Global and Planetary Change, 52, 23–56, https://doi.org/10.1016/j.gloplacha.2006.02.013, 2006.

Bohren, C. F. and Huffman, D. R.: Absorption and Scattering of Light by Small Particles, Absorption and Scattering of Light by Small Particles, https://doi.org/10.1002/9783527618156, 1998.

Chandra, S., Satheesh, S. K., and Srinivasan, J.: Can the state of mixing of black carbon aerosols explain the mystery of 'excess' atmospheric absorption?, Geophysical Research Letters, 31, L19 109, https://doi.org/10.1029/2004GL020662, 2004.

Dalirian, M., Ylisirniö, A., Buchholz, A., Schlesinger, D., Ström, J., Virtanen, A., and Riipinen, I.: Cloud droplet activation of black carbon particles coated with organic compounds of varying solubility, Atmospheric Chemistry and Physics, 18, 12 477–12 489, https://doi.org/10.5194/acp-18-12477-2018, 2018.

Dey, S., Tripathi, S. N., and Mishra, S. K.: Probable mixing state of aerosols in the Indo-Gangetic Basin, northern India, Geophysical Research Letters, 35, L03 808, https://doi.org/10.1029/2007GL032622, 2008.

Dong, Z., Qin, D., Li, K., Kang, S., Wei, T., and Lu, J.: Spatial variability, mixing states and composition of various haze particles in atmosphere during winter and summertime in northwest China, Environmental Pollution, 246, 79–88, https://doi.org/https://doi.org/10.1016/j.envpol.2018.11.101, 2019.

Draine, B. T. and Flatau, P. J.: Discrete-Dipole Approximation For Scattering Calculations, JOSA A, Vol. 11, Issue 4, pp. 1491-1499, 11, 1491–1499, https://doi.org/10.1364/josaa.11.001491, 1994.

Hess, M., Koepke, P., and Schult, I.: Optical Properties of Aerosols and Clouds: The Software Package OPAC, Bulletin of the American Meteorological Society, 79, 831–844, https://doi.org/10.1175/1520-0477(1998)079<0831:OPOAAC>2.0.CO;2, 1998.

Hu, J., Li, J., Tsona Tchinda, N., Song, Y., Xu, M., Li, K., and Du, L.: Underestimated role of sea surface temperature in sea spray aerosol formation and climate effects, npj Climate and Atmospheric Science, 7, 1–12, https://doi.org/10.1038/s41612-024-00823-x, 2024.

Koepke, P., Hess, M., Schult, I., and Shettle, E. P.: Global Aerosol Data Set, Tech. rep., Hamburg, Germany, ISSN 0937-1060, https://search.worldcat.org/title/67711661, 1997.

Koepke, P., Gasteiger, J., and Hess, M.: Technical Note: Optical properties of desert aerosol with non-spherical mineral particles: data incorporated to OPAC, Atmospheric Chemistry and Physics, 15, 5947–5956, https://doi.org/10.5194/acp-15-5947-2015, 2015.

Kojima, T., Buseck, P. R., Iwasaka, Y., Matsuki, A., and Trochkine, D.: Sulfate-coated dust particles in the free troposphere over Japan, Atmospheric Research, 82, 698–708, https://doi.org/10.1016/J.ATMOSRES.2006.02.024, 2006.

Lesins, G., Chylek, P., and Lohmann, U.: A study of internal and external mixing scenarios and its effect on aerosol optical properties and direct radiative forcing, Journal of Geophysical Research: Atmospheres, 107, https://doi.org/10.1029/2001jd000973, 2002.

Li, W., Shao, L., Li, R., Yang, S., Wang, Z., and Tang, U.: Internally Mixed Sea Salt, Soot, and Sulfates at Macao, a Coastal City in South China, Journal of the Air and Waste Management Association, 61, 1166–1173, https://doi.org/10.1080/10473289.2011.603996, 2011.

Li, W., Sun, J., Xu, L., Shi, Z., Riemer, N., Sun, Y., Fu, P., Zhang, J., Lin, Y., Wang, X., Shao, L., Chen, J., Zhang, X., Wang, Z., and Wang, W.: A conceptual framework for mixing structures in individual aerosol particles, Journal of Geophysical Research: Atmospheres, 121, 784–13, https://doi.org/10.1002/2016JD025252, 2016.

https://doi.org/10.5194/egusphere-2026-3777
Preprint. Discussion started: 11 August 2026

Li, W. J. and Shao, L. Y.: Observation of nitrate coatings on atmospheric mineral dust particles, Atmospheric Chemistry and Physics, 9, 1863–1871, https://doi.org/10.5194/acp-9-1863-2009, 2009.

McFiggans, G., Artaxo, P., Baltensperger, U., Coe, H., Facchini, M. C., Feingold, G., Fuzzi, S., Gysel, M., Laaksonen, A., Lohmann, U., Mentel, T. F., Murphy, D. M., O'Dowd, C. D., Snider, J. R., and Weingartner, E.: The effect of physical and chemical aerosol properties on warm cloud droplet activation, Atmospheric Chemistry and Physics, 6, 2593–2649, https://doi.org/10.5194/acp-6-2593-2006, 2006.

Mie, G.: Beiträge zur Optik trüber Medien, speziell kolloidaler Metallösungen, Annalen der Physik, 330, 377–445, https://doi.org/10.1002/ANDP.19083300302, 1908.

Mishchenko, M. I., Hovenier, J. W., and Travis, L. D., eds.: Light scattering by nonspherical particles : theory, measurements, and applications, Elsevier Science, Burlington, ISBN 9780080510200, www.worldcat.org/title/437186724, 1999.

Mishra, S. K., Ahlawat, A., Khosla, D., Sharma, C., Prasad, M. V., Singh, S., Gupta, B., Tulsi, Sethi, D., Sinha, P. R., Ojha, D. K., Wiedensohler, A., and Kotnala, R. K.: Experimental investigation of variations in morphology, composition and mixing-state of boundary layer aerosol: A balloon based study over urban environment (New Delhi), Atmospheric Environment, 185, 243–252, https://doi.org/10.1016/j.atmosenv.2018.04.053, 2018.

O'Dowd, C. D., Facchini, M. C., Cavalli, F., Ceburnis, D., Mircea, M., Decesari, S., Fuzzi, S., Young, J. Y., and Putaud, J. P.: Biogenically driven organic contribution to marine aerosol, Nature, 431, 676–680, https://doi.org/10.1038/nature02959, 2004.

P Raj, S. and Sinha, P. R.: sampr7/AeroMix: v1.0.1, https://doi.org/10.5281/zenodo.10552079, 2024.

P Raj, S. and Sinha, P. R.: Python codes of the analysis presented in 'An analytical formulation of optical inversion modeling of aerosol mixing state using AeroMix v1.0.1', https://doi.org/10.5281/zenodo.21798191, 2026.

Pedrós, R., Gómez-Amo, J. L., Marcos, C. R., Utrillas, M. P., Gandía, S., Tena, F., and Lozano, J. A.: AEROgui: A graphical user interface for the optical properties of aerosols, Bulletin of the American Meteorological Society, 95, 1863–1871, https://doi.org/10.1175/BAMS-D-13-00162.1, 2014.

Raj, S. P., Sinha, P. R., Srivastava, R., Bikkina, S., and Subrahamanyam, D. B.: AeroMix v1.0.1: a Python package for modeling aerosol optical properties and mixing states, Geoscientific Model Development, 17, 6379–6399, https://doi.org/10.5194/gmd-17-6379-2024, 2024.

Scarnato, B. V., Vahidinia, S., Richard, D. T., and Kirchstetter, T. W.: Effects of internal mixing and aggregate morphology on optical properties of black carbon using a discrete dipole approximation model, Atmospheric Chemistry and Physics, 13, 5089–5101, https://doi.org/10.5194/acp-13-5089-2013, 2013.

Sinha, P. R., Manchanda, R. K., Kaskaoutis, D. G., Kumar, Y. B., and Sreenivasan, S.: Seasonal variation of surface and vertical profile of aerosol properties over a tropical urban station hyderabad, India, Journal of Geophysical Research Atmospheres, 118, 749–768, https://doi.org/10.1029/2012JD018039, 2013.

Song, Y., Li, J., Tsona Tchinda, N., Li, K., and Du, L.: Role of sea spray aerosol at the air–sea interface in transporting aromatic acids to the atmosphere, Atmospheric Chemistry and Physics, 24, 5847–5862, https://doi.org/10.5194/acp-24-5847-2024, 2024.

Srivastava, R., Ramachandran, S., and Rajesh, T. A.: Aerosol mixing over an urban region: radiative effects, Quarterly Journal of the Royal Meteorological Society, 142, 1732–1744, https://doi.org/10.1002/qj.2769, 2016.

Strang, G.: Linear Algebra and Its Applications, Academic Press, New York, 2 edn., ISBN 012673660X, http://libraryopac.math.iisc.ac.in/bib/1853, 1980.

Wang, M., Zhu, T., Zhao, D., Rubach, F., Wahner, A., Kiendler-Scharr, A., and Mentel, T. F.: Cloud condensation nuclei activity of CaCO 3 particles with oleic acid and malonic acid coatings, Atmospheric Chemistry and Physics, 18, 7345–7359, https://doi.org/10.5194/acp-18-7345-2018, 2018.

https://doi.org/10.5194/egusphere-2026-3777
Preprint. Discussion started: 11 August 2026

Waterman, P. C.: Symmetry, Unitarity, and Geometry in Electromagnetic Scattering, Physical Review D, 3, 825, https://doi.org/10.1103/PhysRevD.3.825, 1971.